

## Picture of the Month

### Tetralogy of Fallot: evaluation by 4D spatiotemporal image correlation

L. GINDES and R. ACHIRON

Department of Obstetrics and Gynecology, The Chaim Sheba Medical Center, Tel Hashomer, Affiliated with the Sackler Faculty of Medicine, Tel Aviv University, Israel

Tetralogy of Fallot (TOF) is the leading cause of cyanotic congenital heart disease among newborns. TOF occurs in approximately 1 in 3600 live births and accounts for 3.5–10% of infants born with congenital heart disease<sup>1,2</sup>. The incidence of TOF in fetuses is unknown.

TOF includes four components: 1) pulmonary artery stenosis (PS); 2) malalignment ventricular septal defect (VSD); 3) displacement of the aorta to the right (allowing it to override the VSD); and 4) hypertrophy of the right ventricle. The right ventricular hypertrophy occurs only after delivery, when the afterload of the right ventricle increases. PS is not always present at early ultrasound examination, and this finding can develop or worsen during pregnancy<sup>3,4</sup>. Thus, in second-trimester fetuses, two components of TOF can be recognized: the VSD and the overriding of the aorta. Routine examination of the four-chamber view may detect the VSD and the left deviation of the heart, but some TOF cases can be missed. Extended cardiac examination, which includes evaluation of the outflow tracts, has been shown by Achiron *et al.*<sup>5</sup> and Benacerraf *et al.*<sup>6</sup> to increase the detection rate of TOF.

The classical two-dimensional rotational and sweep techniques of fetal echocardiography are only able to demonstrate the TOF features in separate sagittal images<sup>7,8</sup>. However, it has been demonstrated that the technique of 4D echocardiographic spatiotemporal image correlation (STIC) allows visualization of the coronal, axial and sagittal cardiac planes, as well as demonstration of the heart as a rendered volume<sup>9,10</sup>.

In the present case we report a 4D STIC rendering of a 25-week fetus with TOF. Figure 1 depicts grayscale STIC of the left outflow tract in the coronal plane: the aorta overriding the malalignment VSD and a small pulmonary artery can be seen. The volume dataset was acquired with axial sweeps through the fetal chest using the STIC technique. Three-dimensional reconstruction was performed with 'gradient light' algorithms. Low threshold and transparency levels were adjusted until the structures of interest were visualized. In this particular case, the transparency

level was set to 50, and the low threshold level to 25 (both scales range from 0 to 250). 4D rendering of this image can be downloaded from the Journal's website (Videoclip S1). This image demonstrates the advantage of the 4D technique that allows presentation of data obtained from multiple sections to be displayed on a rendered image.

Figure 2 shows the manipulation of the same volume with inversion mode. This rendering algorithm transforms echolucent structures into solid voxels<sup>11–13</sup> and allows better tracing of blood vessels. Our ability to transform the same volume data set, using different algorithms such as inversion mode, allows different aspects of the anomaly

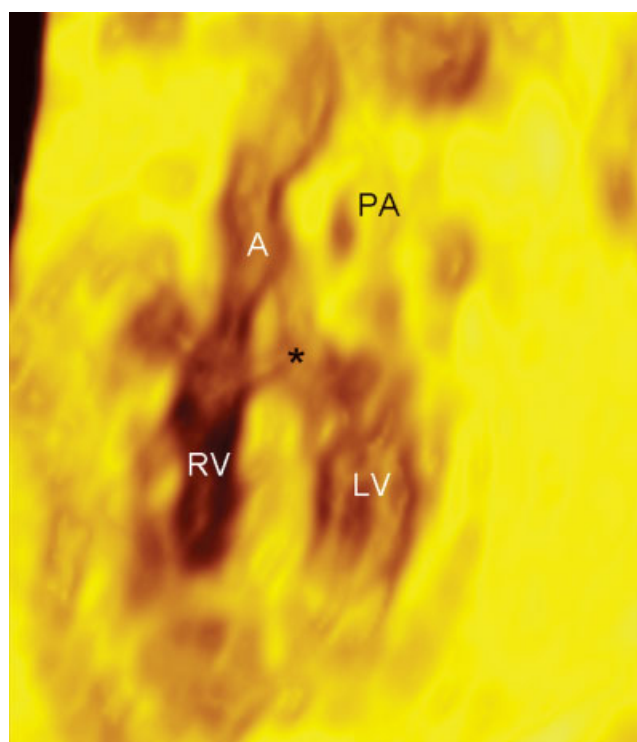


**Figure 1** Grayscale spatiotemporal image correlation of the left outflow tract of a 25-week fetus with tetralogy of Fallot. The aorta (A) is overriding on the interventricular septum, that has a membranous ventricular septal defect (\*). RV, right ventricle; LV, left ventricle; PA, pulmonary artery.

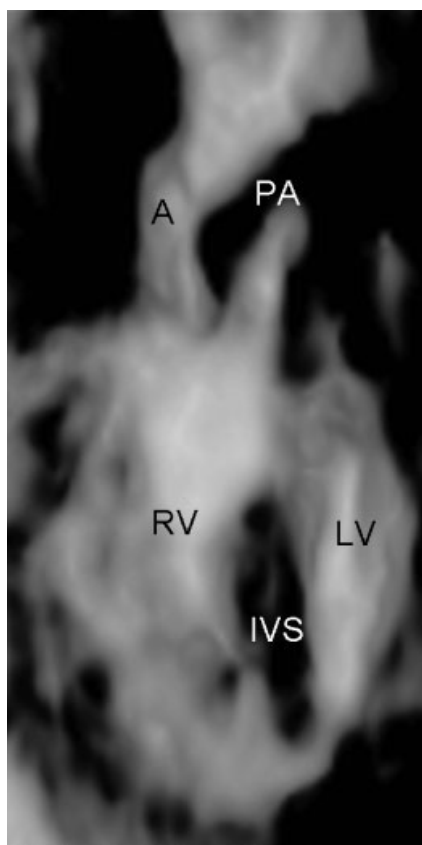


**Figure 2** Combination of spatiotemporal image correlation and inversion mode for the diagnosis of the same case as shown in Figure 1 (25-week fetus with tetralogy of Fallot). A, aorta; RV, right ventricle; LV, left ventricle; PA, pulmonary artery; IVS, interventricular septum.

that are usually indiscernible by regular rendering, to be revealed. In TOF the demonstration of the whole course of the pulmonary artery and aorta enables the prognosis of the anomaly to be defined. The pulmonary artery to aorta ratio may predict the severity of the disease<sup>3,14</sup>. 4D rendering of this image can also be downloaded from the Journal's website (Videoclip S2).

In conclusion, we have described the application of 4D STIC acquisition with post processing reconstruction with 'gradient light' and 'inversion mode' algorithms. These diverse modes provide different information that may be valuable in the evaluation of congenital heart disease.

## References

1. Shinebourne EA, Babu-Narayan SV, Carvalho JS. Tetralogy of Fallot: from fetus to adult. *Heart* 2006; **92**: 1353–1359.
2. Yoo SJ, Lee YH, Kim ES, Ryu HM, Kim MY, Yang JH, Chun YK, Hong SR. Tetralogy of Fallot in the fetus: findings at targeted sonography. *Ultrasound Obstet Gynecol* 1999; **14**: 29–37.
3. Lee W, Smith RS, Comstock CH, Kirk JS, Riggs T, Weinhouse E. Tetralogy of Fallot: prenatal diagnosis and postnatal survival. *Obstet Gynecol* 1995; **86**: 583–588.
4. Yagel S, Weissman A, Rotstein Z, Manor M, Hegesh J, Anteby E, Lipitz S, Achiron R. Congenital heart defects: natural course and in utero development. *Circulation* 1997; **96**: 550–555.
5. Achiron R, Glaser J, Gelernter I, Hegesh J, Yagel S. Extended fetal echocardiographic examination for detecting cardiac malformations in low risk pregnancies. *BMJ*. 1992; **304**: 671–674.
6. Benacerraf BR. Sonographic detection of fetal anomalies of the aortic and pulmonary arteries: value of four-chamber view vs direct images. *AJR Am J Roentgenol* 1994; **163**: 1483–1489.
7. DeVore GR. The aortic and pulmonary outflow tract screening examination in the human fetus. *J Ultrasound Med* 1992; **11**: 345–348.
8. Yagel S, Cohen SM, Achiron R. Examination of the fetal heart by five short-axis views: a proposed screening method for comprehensive cardiac evaluation. *Ultrasound Obstet Gynecol* 2001; **17**: 367–369.
9. Yagel S, Cohen SM, Shapiro I, Valsky DV. 3D and 4D ultrasound in fetal cardiac scanning: a new look at the fetal heart. *Ultrasound Obstet Gynecol* 2007; **29**: 81–95.
10. Paladini D, Vassallo M, Sglavo G, Lapadula C, Martinelli P. The role of spatio-temporal image correlation (STIC) with tomographic ultrasound imaging (TUI) in the sequential analysis of fetal congenital heart disease. *Ultrasound Obstet Gynecol* 2006; **27**: 555–561.
11. Gonçalves LF, Espinoza J, Lee W, Mazor M, Romero R. Three- and four-dimensional reconstruction of the aortic and ductal arches using inversion mode: a new rendering algorithm for visualization of fluid-filled anatomical structures. *Ultrasound Obstet Gynecol* 2004; **24**: 696–698.
12. Espinoza J, Gonçalves LF, Lee W, Mazor M, Romero R. A novel method to improve prenatal diagnosis of abnormal systemic venous connections using three- and four-dimensional ultrasonography and 'inversion mode'. *Ultrasound Obstet Gynecol* 2005; **25**: 428–434.
13. Ghi T, Gera E, Segata M, Michelacci L, Pilu G, Pelusi G. Inversion mode spatio-temporal image correlation (STIC) echocardiography in three-dimensional rendering of fetal ventricular septal defects. *Ultrasound Obstet Gynecol* 2005; **26**: 679–680.
14. Achiron R, Golan-Porat N, Gabbay U, Rotstein Z, Heggesh J, Mashiach S, Lipitz S. *In utero* ultrasonographic measurements of fetal aortic and pulmonary artery diameters during the first half of gestation. *Ultrasound Obstet Gynecol* 1998; **11**: 180–184.

## SUPPORTING INFORMATION ON THE INTERNET

The following supporting information may be found in the online version of this article:

**Videoclip S1** Grayscale spatiotemporal image correlation of the left outflow tract of a 25-week fetus with tetralogy of Fallot. This anterior view demonstrates the ventricular and atrial contraction, the large ventricular septal defect, the dilated and overriding aorta and the mitral and tricuspid valves. The narrow pulmonary artery is only partially demonstrated.

**Videoclip S2** Combination of spatiotemporal image correlation and inversion mode for the diagnosis of the same case as shown in S1 (25-week fetus with tetralogy of Fallot). The anterior narrow pulmonary artery is demonstrated coming out of the right ventricle, the posterior wide aorta and the left ventricle are also seen, but the ventricular septal defect and overriding aorta cannot be detected in this videoclip.